

# Numerical modelling of Alpine deep flow systems: a management and prediction tool for an exploited geothermal reservoir (Lavey-les-Bains, Switzerland)

Romain Sonney · François-David Vuataz

**Abstract** The geothermal site of Lavey-les-Bains, Switzerland is an Alpine deep flow system in fractured crystalline rocks. Groundwater analyses since 1973 reveal a mixing process between a deep warm component (68°C and TDS 1.4g/L) and cold shallow water. The production rate of the new deep well P600, installed in 1997, has amplified this mixing process in well P201, for which a decline in temperature and TDS has been observed. Numerical hydrogeological two-dimensional and three-dimensional models of heat, flow and mass transport have been developed to reproduce the geothermal system and to forecast the long-term exploitation potential of the geothermal resource. The computed temperature of the deep inferred reservoir (100–130°C) is in agreement with the geothermometers, whereas the simulated thermal water flux (5,400–9,000m<sup>3</sup>/day) is probably underestimated. Different fluid production scenarios can reproduce the decline and stabilization phases of temperatures in the geothermal field since 1997. For P201, the mixing ratio calculated before and during the exploitation of P600 is comparable with observed data; the modelled temperature tends towards stabilization in P201 at 56°C after 10–15years of production at P600. Another proposed new well is likely to reduce the thermal output of the existing wells.

**Keywords** Alpine hydrothermal system · Groundwater management · Crystalline rocks · Mixing processes · Switzerland

## Introduction

Alpine deep flow systems have not been the subject of numerical modelling even if the majority of them have

been thoroughly studied. Geothermal reservoirs in the Alpine range are partially exploited at some spas. Emergence temperatures of thermal water, which correspond either to springs or boreholes, vary between 15 and 65°C for the warmest thermal water in the Swiss Alps (Lavey-les-Bains) with discharges ranging between <1 and 35 L/s (Sonney and Vuataz 2008). Over-exploitation of thermal water usually generates important decreases of temperature and mineralization due to mixing processes with cold-water inflow, and creates problems for sustainable long-term exploitation. In Lavey-les-Bains, the spa has encountered this inconvenience since 1997 with the beginning of the exploitation of a new deep borehole (P600). The loss of a few degrees of temperature raises questions about the exploitation rate and it was considered important to quantify cold groundwater inflows and visualize the long-term evolution of temperature with numerical methods. Two dimensional and three-dimensional models of flow, heat and mass transport were undertaken to represent the initial hydrogeological conditions and to manage the long-term exploitation of the geothermal resource, using a coupled numerical simulation code (FEFLOW).

A geothermal project, Alpine Geothermal Power Production (AGEPP) began in 2006 with the objective to generate electricity and heat by drilling into the Lavey-les-Bains geothermal reservoir with a proposed 2.5–3 km deep borehole. The feasibility study of the AGEPP project evaluated that the characteristics of this potential reservoir are economically interesting: fractured permeability, reservoir fluid temperature around 100–110°C, a production yield of 50–75 L/s and a weak mineralization of the deep fluid (G. Bianchetti, Alpgeo Ltd., unpublished data, 2006). The presently reported study considers the future borehole by including it in the three-dimensional model to show its potential impact on the two existing production wells.

## Location, history and exploitation of thermal waters

The geothermal zone of Lavey-les-Bains is located in the Rhone Valley within the Western External Alps of Switzerland, 15 km upstream from Lake Geneva and

Received: 18 March 2008 / Accepted: 30 October 2008  
Published online: 27 November 2008

© Springer-Verlag 2008

R. Sonney (✉) · F.-D. Vuataz  
Centre for Geothermal Research - CREGE, c/o CHYN,  
University of Neuchâtel,  
E. Argand 11, CP 158, 2009, Neuchâtel, Switzerland  
e-mail: [romain.sonney@crege.ch](mailto:romain.sonney@crege.ch)  
Tel.: +41-32-7182692  
Fax: +41-32-7182603

2 km from the city of Saint-Maurice (canton of Wallis) on the NE bank of the Rhone River (Fig. 1). Morphologically, the studied zone is located on the Rhone alluvial deposits, compressed between the front of a fan delta and rock-falls from the mountain slope of the Dent de Morcles. The old well “P201” (depth of 201 m) and the new well “P600” (595-m inclined borehole) are used by the spa. Uprising thermal waters from a fractured gneiss of the Aiguilles Rouges Massif are pumped continuously. On the site, one old exploitation well, exploratory boreholes and piezometers are mainly gathered around P201 well and their depths vary between 10 and 250 m (Fig. 2). A divergence tunnel of the Lavey hydropower plant deflects part of the Rhone River water and also drains some cold springs.

The thermal spring of Lavey-les-Bains was discovered in 1831 emerging in the Rhone bed, on its NE bank. The

first works for collecting thermal water were installed in 1832 with the old well “AP” (Ancien Puits in French) to be used for developing the known thermal spa, located 300 m downstream from the thermal zone (Zahner et al. 1974). Since then, the natural spring has disappeared in the alluvial deposits. In 1972, the installation of a 201 m deep borehole (P201), at 50 m approximately upstream from AP, allowed thermal waters at 62°C to be pumped with a maximum flow of 450 L/min from the fractured gneiss (Vuataz 1982; Bianchetti 1994). The borehole P600 was drilled in 1997 with the aim to increase temperature and production rate, and to guarantee the thermal energy autonomy of the new spa (swimming pools, heating, ventilation and production of hot water for medical purposes) without using heat pumps or fossil fuels (G. Bianchetti, Alpgeo Ltd., unpublished data, 2002). The exploitation of water in the P600 well is generally carried

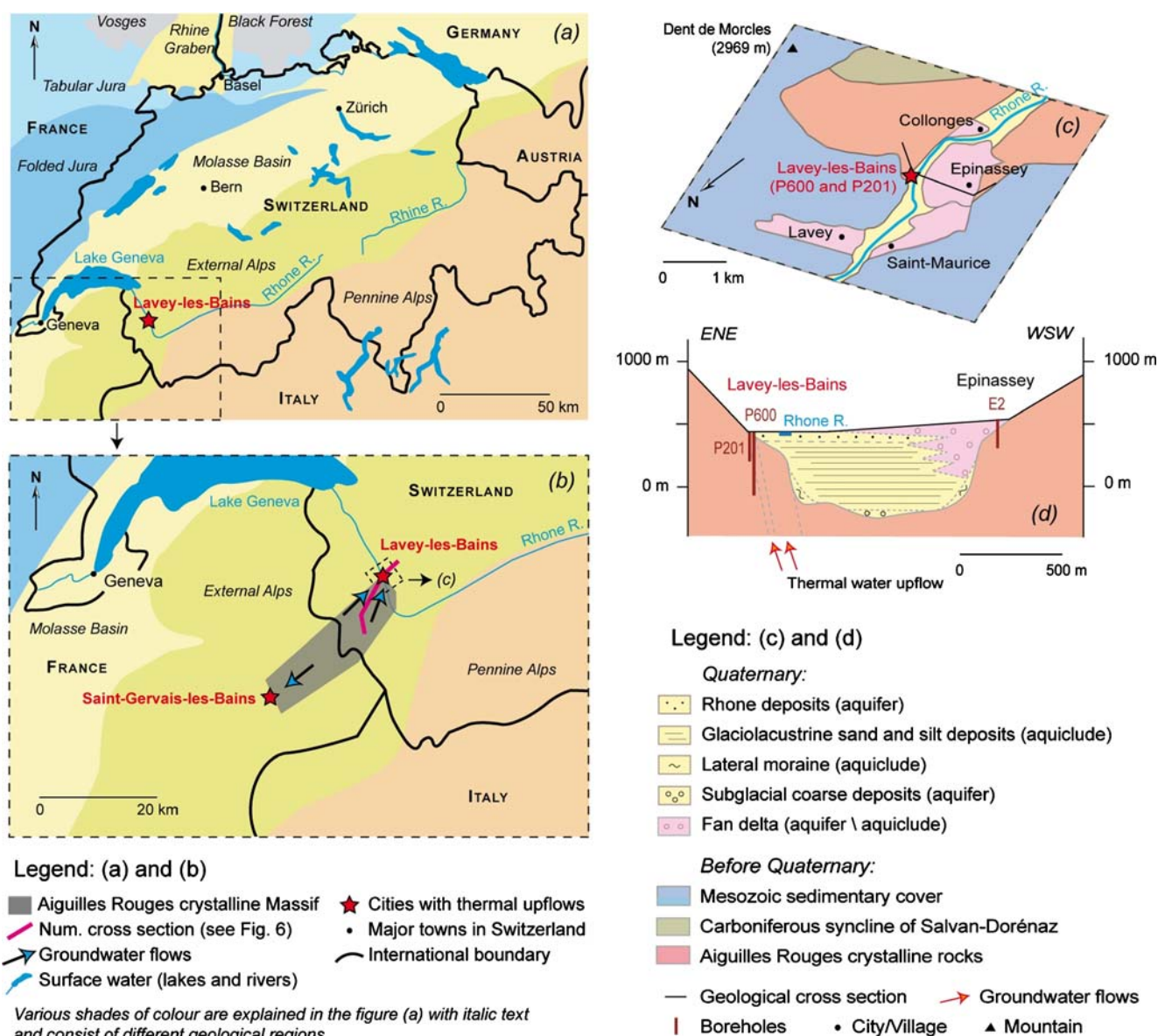


**Fig. 1** a–b Geographical location of Lavey-les-Bains in Switzerland. b–c Regional and local geological settings on the NE part of the Aiguilles Rouges crystalline Massif. d Two-dimensional numerical cross section of the Quaternary filling in the Lavey-les-Bains area

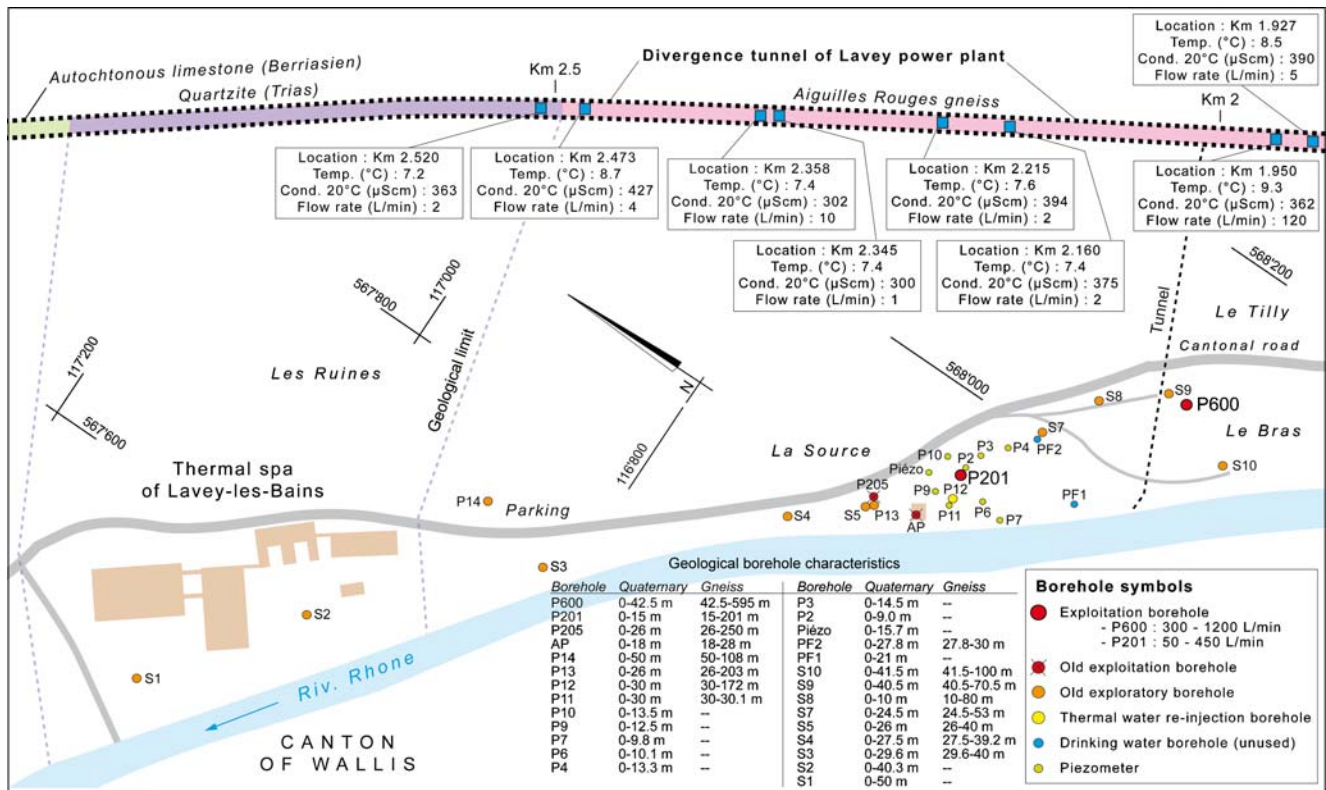


**Fig. 2** Location map and characteristics of the wells and piezometers in the spa area and of the springs in the divergence tunnel of Lavey power plant. Location refers to the Swiss kilometric coordinates in projection, in standard CH1903

out by alternate periods of high pumping rates (close to 1,200 L/min especially in winter), followed by phases of low pumping rates (close to 300 L/min mainly during the summer season). Simultaneously, the well P201 is pumped under a regular mode all year round with pumping rates ranging between 200 and 450 L/min.

## Hydrogeological setting

### Regional deep flow system

Two types of aquifer coexist in the studied area: aquifers with interstitial porosity like alluvial and glacial groundwaters of the Rhone Valley and aquifers with fracture porosity. Concerning aquifers with fracture porosity, groundwater circulates inside fissures of gneiss of the Aiguilles Rouges Massif (Bianchetti 1994). Infiltration and circulation within these high reliefs take place from SW to NE, via Variscan and Alpine geological structures (Lhomme et al. 1996; Von Raumer and Bussy 2004). Knowing that the spa of Lavey-les-Bains is located on the right bank of the Rhone Valley, whereas the watershed area is on the left bank, waters collected in Lavey-les-Bains have to circulate at depth below the glacioluvial Quaternary deposits. In the south-western part of the Aiguilles Rouges Massif, groundwaters flow towards the south-west (Fig. 1). The thermal springs of Saint-Gervais-

les-Bains (France) show again the presence of uprising deep fluid, with discharge temperatures up to 40°C (Vuataz 1982).

The deep reservoir of the regional flow system could be located at 2,500 m below sea level. It corresponds to the overthrust fault of the Aiguilles Rouges Massif on the Infra Aiguilles Rouges Massif according to the interpretation of a seismic profile passing by Lavey-les-Bains (Pfiffner et al. 1997). Using geochemical modelling of water-rock interaction as well as the calculation of chemical geothermometers (Nicholson 1993), the maximum temperature of the potential reservoir is estimated around 100–110°C (Bianchetti 1994). Finally, stable isotope studies allowed calculation of the average elevation of infiltration at 1,700–2,100 m and carbon-14 analyses resulted in an average residence time older than 8000 years (unpublished data).

### Local hydrogeological setting

In the zone of the geothermal boreholes, cracks of NNW–SSE extension and NE–SW brecciated faults meet, which drain the uprising deep fluid towards the Rhone alluvial deposits (Figs. 1 and 4). Shallow groundwater flows take place mainly inside the upper part of the Quaternary filling because the glaciolacustrine deposits have a low permeability and thus are compared to an aquiclude. However, some circulation can also exist in fan deltas and in



subglacial coarse deposits, which are probably more permeable (Fig. 1).

Waters of Lavey-les-Bains area can be subdivided into three hydrogeochemical families defining different mixing end-members (Figs. 3 and 4; Table 1):

- *Sodium-sulphate and chloride thermal waters.* Waters of P600 and P201 are characteristic of this geochemical type and represent the deep thermal crystalline component slightly mixed with shallow groundwater (Fig. 4). The TDS ranges around 1.3–1.5 g/L and the main chemical compounds considered as natural markers are Li, Na, K, Cl, SO<sub>4</sub>, F and SiO<sub>2</sub>. Sulphates mainly come from the oxidation of diffuse sulphides (pyrite) contained in the gneisses (Bianchetti 1994), without completely excluding the influence of Triassic rocks (gypsum) at depth.
- *Calcium-bicarbonate cold waters.* Rhone River water and alluvial groundwater are characteristic of this family and are much less mineralized (TDS 100–300 mg/L) than the thermal water. Ca, Mg, HCO<sub>3</sub> and tritium are the representative elements of this component.

– *Calcium-bicarbonate subthermal and cold groundwaters.* They are springs in the gallery of the Lavey power plant and water from the S9 exploratory borehole. This family corresponds to waters having circulated at shallow depth in the gneiss of the slope of the Dent de Morcles Massif (Fig. 4). This component is similar to the Rhone alluvial groundwater with the same representative elements but with a stronger mineralization (TDS 300–400 mg/L).

On the thermal site, various mixing processes are observed between these three families of water (Fig. 4). The evolution from the warm end-member to the cold end-member is marked by a reduction in Li, Na, K, Cl, SO<sub>4</sub>, F and SiO<sub>2</sub>, compensated by an increase in Ca, Mg, HCO<sub>3</sub> and tritium. This evolution is also accompanied by a decrease of the total mineralization and of the temperature. Water chemical analyses of the deeper boreholes in August 2007 (P600, P201, P205, P13, S8 and S9) show good correlations between chloride, sulphate and magnesium (Fig. 3). These boreholes, which are screened only into the gneissic massif,

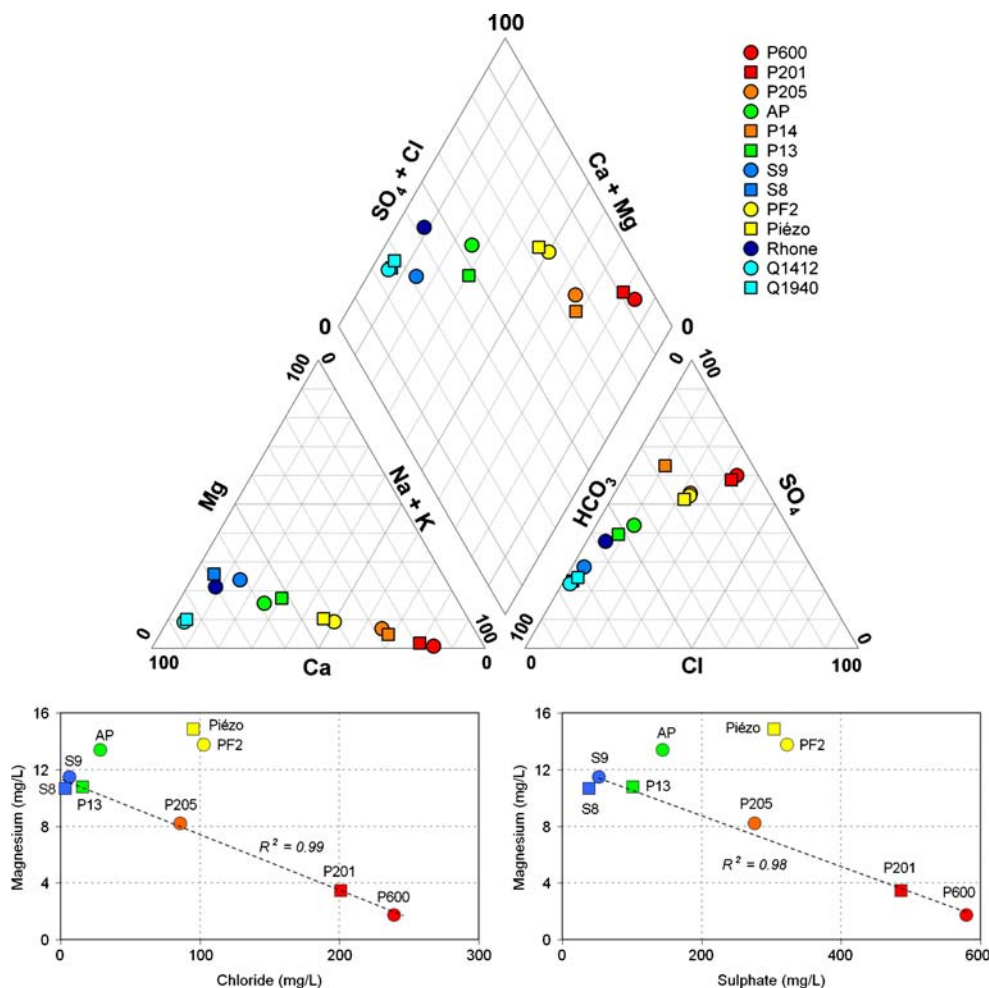


**Fig. 3** Piper diagram of the waters of Lavey-les-Bains area and composition plots for the deep boreholes. Locations of the samples are shown in Fig. 2; Q1412 and Q1940 are springs in the divergence tunnel of Lavey power plant which were sampled (numbers 1412 and 1940 represent their location in meters). Data used for these plots come from the one-off sampling rounds described in Table 1, not averages of values

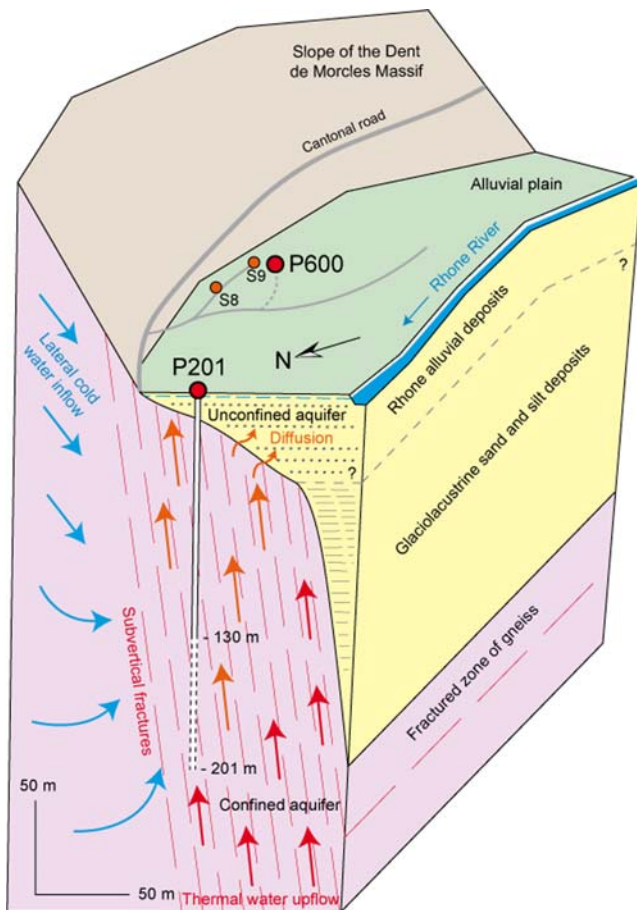


**Fig. 4** Conceptual three-dimensional diagram of the hydrodynamic context of the Lavey-les-Bains geothermal system, showing the different hydrostratigraphic units and the mixing process between lateral cold-water inflow and ascending deep fluid. The legend for symbols of boreholes is illustrated in the Fig. 2. The P201 well is screened between 130 and 201 m

are not influenced by infiltrations from the Rhone alluvial aquifer. In return, the old well AP, which is much shallower (28 m) and close to the Rhone River contains some alluvial groundwater. In the unused well PF2, crossing only the Quaternary deposits, higher values of electrical conductivity (about 1,200  $\mu\text{S}/\text{cm}$ ) were measured, and are due to the rejection of surplus P600 water directly into the alluvial groundwater (thermal water plume). Before this rejection, electrical conductivity in PF2 was around 400  $\mu\text{S}/\text{cm}$ .

### Long-term variations of physico-chemical parameters

Since 1997, the exploitation of the P600 well has generated a significant decrease of temperature and electrical conductivity in thermal waters due to an increase of the mixing process. Measurements at the P201 well show a decrease of these parameters between 1997 and 2001: from 62 to 57°C and 1,800 to 1,300  $\mu\text{S}/\text{cm}$ , respectively. For P600, this diminution is less pronounced: from 68 to 65°C and 2,000 to 1,700  $\mu\text{S}/\text{cm}$  (Fig. 5). One also notes that concentration of

major ions in P201 decrease significantly after 1997, with the exception of magnesium and bicarbonate, natural tracers of the cold water. Moreover, tritium analyses of groundwater from the two wells (unpublished data) show the existence in P600 of a small component of groundwater infiltrated after the first nuclear tests in 1953 ( $1 \text{ tritium units (TU)} \pm 0.5$ ) and a more important aquifer mixing in well P201 ( $2.3 \text{ TU} \pm 0.4$ ). In detail, the diminution of conductivity shows seasonal cycles due to different pumping cycles. During winter, higher pumping rates increase the mixing process with cold waters circulating at shallow depth in the gneiss, and measured temperatures as well as conductivities are lower (Fig. 5). The annual average temperature in P600 and P201 wells continued to drop between 2001 and 2005 but not as significantly as the period 1997–2001. It is difficult to explain why conductivity is stabilized after 2001, whereas the temperature continued to decrease slowly up to 2005. It probably corresponds to heat exchanges by advection-diffusion due to modification of exfiltration velocities from the deep reservoir, or effects caused by the variation of recharge in the infiltration area (melt of glaciers). The thermal aquifer is not overexploited in terms of water quantity because the static and dynamic water level in the production wells is globally stable.

## Heat and flow groundwater modelling

### Introduction

Long-term data of geothermal fields under production are a precious source of information for numerical modelling. They contribute to the understanding of the heat, mass and chemical transfer processes in geothermal reservoirs and allow one to better estimate the resource. With the development of computer simulation tools since the 1990s, numerous studies including numerical models applied to geothermal systems have proliferated. Applications generated by diverse functionalities of these models are varied: two-dimensional or three-dimensional imaging of a geothermal system using stochastic methods (Teng and Koike 2007), fluid production and reinjection scenarios (Kühn and Stöfen 2004; Porras et al. 2007), water-rock interactions (Dobson et al. 2004; Gevrek 2000), hydraulic connection with a deeper geothermal reservoir (Flores-Marquez et al. 2006), variation of local effective thermal stress (McDermott et al. 2006), and other applications concerning enhanced geothermal systems (André et al. 2006; Kohl et al. 1995; Kolditz and Clauser 1998; Pruess 2006).

### Two-dimensional vertical modelling of groundwater heat and flow transports

Until now, no numerical models have been constructed for the Lavey-les-Bains hydrothermal system. The first step was to build a simplified two-dimensional numerical model through the Aiguilles Rouges Massif based on a regional NNE–SSW cross section (Figs. 1 and 6). Initial conditions of groundwater flow and heat transport were

**Table 1** Chemical composition of selected waters sampled of Lavey-les-Bains

Borehole/spring	P600	P201	AP	P13	Pièzo	S9	S8	PF2	P14	P205	Rhone R.	Q1412	Q1940
Sampling date	30.08.07	30.08.07	30.08.07	30.08.07	30.08.07	31.08.07	31.08.07	31.08.07	31.08.07	15.03.90	16.08.90	17.01.85	17.01.85
Laboratory/reference	CHYN	CHYN	CHYN	CHYN	CHYN	CHYN	CHYN	CHYN	CHYN	Bianchetti <sup>a</sup>	Data from Bianchetti <sup>a</sup>	Data from CRSFA <sup>b</sup>	Data from CRSFA <sup>b</sup>
In situ measurements													
Temp. pumping end (°C)	65.3	56.8	19.7	23.3	14.6	26.5	18.7	15.1	18.9	33.0	7.5	12.4	9.3
Air temp. (°C)	18	18	18	18	18	15	20	22	22	15	19		
EC, 25°C (µS/cm)	1,984	1,709	676	513	1,167	380	328	1,229	767	907	118	392	383
pH	7.56	7.41	7.69	7.17	7.30	7.22	7.65	7.40	7.93	7.59	8.39	(20°C)	(20°C)
Oxygen (%)	0.3	1.9	39.3	32.9	70.8	3.4	38.5	57.9	0.8				6.30
Oxygen (mg/L)	0.01	0.09	3.25	2.55	6.35	0.25	3.25	5.22	0.07				
Corrected Eh (mV)	-50	-56	466	233						-215	175		
Flow (L/min)	≈ 300	≈ 450	17	24	≈ 15	16	7	15	16	300		120	180
Pump depth (m)	≈ 93	≈ 50	≈ 12	≈ 15	≈ 10	≈ 18	≈ 15	≈ 15	≈ 12				
Final drawdown (m)		29.30	7.12	8.95	6.67	15.34	14.01	11.96	7.49				
Analyses													
Calculated TDS (mg/L)	1,410	1,207	527	576	836	299	272	866	555	774	95	352	352
Ca	57.2	60.5	82.4	53.8	102.7	48.9	46.6	99.8	38.5	54.8	15.7	84.4	79.4
Mg	1.74	3.45	13.4	10.8	14.8	11.5	10.7	13.8	4.22	8.2	2.9	5.5	5.7
Na	360	288	40.2	34.2	124	11.9	3.89	139	112	146	1.6	5	5
K	11.20	9.46	3.04	2.81	4.55	2.45	1.17	4.72	3.49	5.9	1.0	2	2
Li	3.23	2.54	0.32	0.33	0.85	0.67	0.016	0.97	0.68	1.30	0.004	c	c
Sr	2.55	1.42	1.66	0.55	NA	1.23	0.63	NA	1.18	1.60	0.3	c	c
HCO <sub>3</sub>	79.7	92.6	197	170	194	162	153	185	120	153	45	214	200
SO <sub>4</sub>	580	486	144	102	300.3	52.7	38	319.5	227	276	23	37.6	54
Cl	239	201	28.5	15.7	94.0	5.06	3.22	101.8	27.7	86.0	2.6	3.9	5.9
F	6.2	4.55	0.84	1.29	1.35	2.15	0.93	1.50	2.87	3.80	0.2		
Br	1.28	1.13	NA	NA	NA	NA	NA	NA	NA	1.08	0.023		
SiO <sub>2</sub>	68.2	56.5	15.4	15.1	19.8	22.6	13.6	21.3	17.9	35.9	2.5		
Cation (meq/L)	19.44	16.48	7.12	5.19	11.96	4.09	3.42	12.40	7.34	10.13	1.12	4.93	4.70
Anion (meq/L)	20.47	17.55	7.08	5.41	12.15	4.01	3.44	12.63	7.63	10.88	1.30	4.39	4.57
Difference (%)	-2.6	-3.2	0.3	-2.1	-0.8	1.0	-0.3	-0.9	-1.9	-3.5	-7.2	5.8	1.4

All sampling points are wells and boreholes except for the Rhone River and the two springs Q1412 and Q1940, which are located in the divergence tunnel of Lavey power plant (see Fig. 2). Data for samples P205, Rhone River, Q1412 and Q1940 come from previous analyses due to difficulties or impossibilities of sampling encountered at the time of the one-off sampling round in August 2007. EC electrical conductivity

<sup>a</sup>G. Bianchetti, Alpege Ltd., unpublished data, 1993

<sup>b</sup>CRSFA, unpublished data, 1992

<sup>c</sup>Estimated value for Na and K



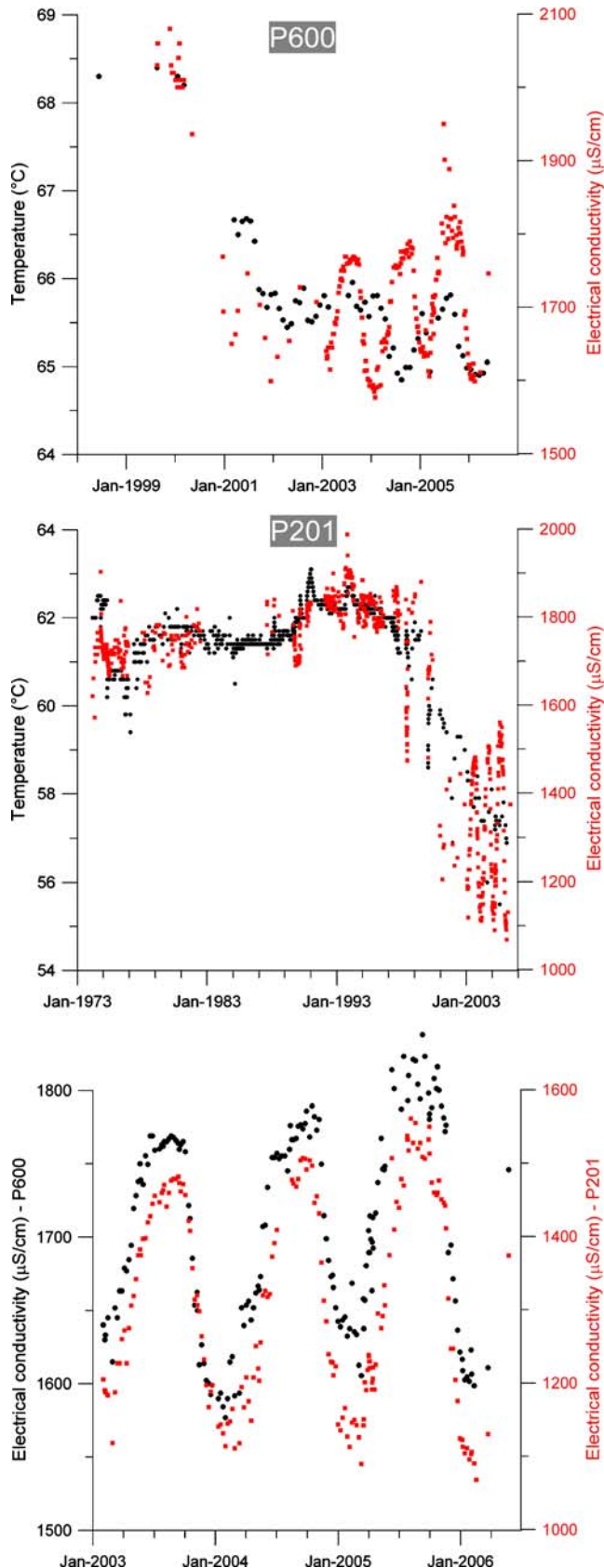


Fig. 5 Variations of temperature and electrical conductivity in the two exploitation wells

calibrated by using data from literature and borehole measurements. Desired aims are:

- To represent the deep flow system from the infiltration area to the Rhone Valley using water fluxes at the top of the domain and rock permeability contrasts
- To simulate the Lavey-les-Bains geothermal anomaly by using a heat flux at the bottom of the model and initial surface temperatures
- To compare the results with observations on the field: temperature in wells, geothermal gradient, temperature in the deep potential reservoir, groundwater balance and residence time of thermal water
- To quantify the uprising water flux
- To represent effects of pumping rates on temperatures and to predict their long-term evolution for an optimal management scenario of this geothermal resource

#### Geological boundary conditions

The two-dimensional numerical model integrates all geological horizons on a 3,000 m thickness below the Rhone Valley, considered as the base of the fluid circulation and linked to the presence of the overthrust fault (Bianchetti 1994). The prolongation of this fault towards the southwest is difficult to evaluate, so it was decided to keep this depth in the model and to assume it as the deep limit (Fig. 6).

The numerical model stops in the NE part near the sedimentary cover below the Dent de Morcles. Towards the SW, the limit is fixed after the Vallorcine shear zone and its granite. It was regarded as a low-permeability limit because of the high compaction and different orientations of its fractures. Admittedly, waters contained inside the sedimentary nappe of Morcles circulate towards the north and east and they probably do not arrive in the Lavey-les-Bains area (Bianchetti 1994; Zahner et al. 1974).

Below the Quaternary filling, the two-dimensional vertical model takes into account the existence of a large fractured zone which is encountered during drilling (Fig. 6) and which allows a fast uprise of the deep fluid towards the surface. The Quaternary filling was subdivided into three parts: the permeable Rhone alluvial deposits, the glaciolacustrine deposits (aquiclude) and the Epinassey fan delta. Lateral moraines and subglacial deposits are not represented in the model because they are very limited (Parriaux and Nicoud 1993).

Concerning the gneissic massif, the infiltration is more important in the decompressed zone than the deep gneiss due to permeability contrast (Cruchet 1985). The evaluation of the proportion of waters which really infiltrate inside the deep gneisses is difficult. The thickness of the decompressed zone varies between 500 and 600 m (Cruchet 1985; Maréchal 1998, 1999) and does not represent a strict limit (not represented in Fig. 6 but considered in the model). This zone can contain important quantities of cold water which are drained towards the base of mountain slopes (Lhomme et al. 1996).

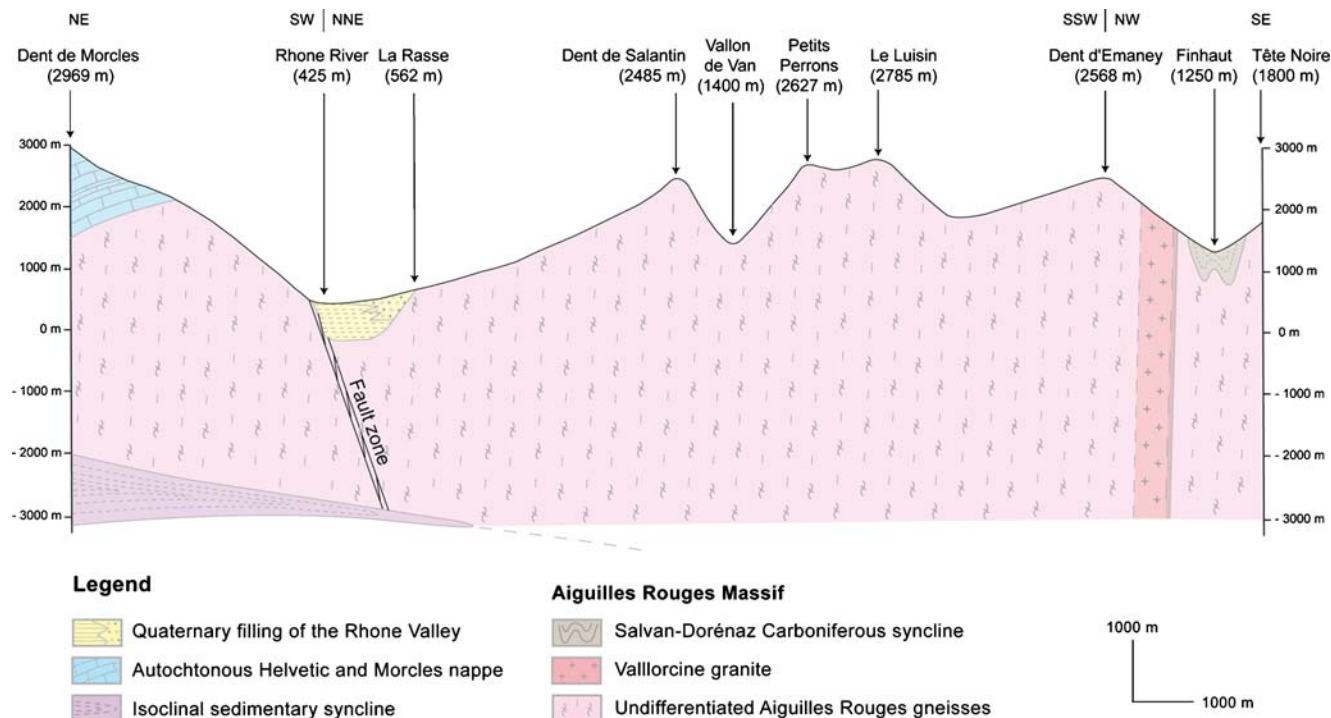


**Fig. 6** Geological cross section of the two-dimensional model for heat and flow transport in the Aiguilles Rouges crystalline Massif (see Fig. 1b). This cross section has two small changes of directions for reason of convenience and for crossing the Vallorcline granite (shear zone), which has the same general orientation as the gneiss

Finally, three important valleys are cut by the cross section of which the Rhone Valley has the lowest elevation. The two other valleys are located between the Dent de Salantin and the Dent d'Emaney with an elevation higher than 1,400 m.a.s.l. (Fig. 6).

#### Assigned parameters

Assigned parameters in the two-dimensional numerical model of groundwater flow and heat transport are described in Table 2. Observed and estimated values come from borehole measurements, literature and from the Swiss Federal Office of Meteorology and Climatology. Imposed water flux does not correspond to a head boundary but to a specific recharge boundary. Water flux is estimated from precipitation, by removal of the effective evapotranspiration and the surface runoff. In short, the effective average groundwater recharge has been evaluated roughly at 10% of precipitation. This relatively low value is due to the importance of runoff, developed in high mountain areas due to the accentuated topography.

The geographical distribution of water fluxes concerns the Petits Perrons and the Dent d'Emaney domains. Flux values fluctuate within an interval from 10% of 1,500 mm/year (median value for the Vallon de Van Valley) to 10% of 2,000 mm/year (median value for mountain tops). For the crystalline rocks below the Morcles sedimentary formations, the imposed flux corresponds to cold waters which are partially found in pumped waters of wells and

in the springs of the divergence tunnel of the Lavey hydro-power plant.

Values of imposed hydraulic conductivities are given in the Table 2 and can be comparable to literature data and results of pumping tests. A hydraulic conductivity anisotropy factor was assigned for several geological units while indicating to the model the contrast of permeability in the X and Y directions with an angle. Consequently, it was possible to reproduce the preferential flows inside the geological units as for the fractured zone of gneiss below the Rhone Valley (Table 2).

Surface temperatures were assigned to the top of the domain from data of the Swiss Federal Office of Meteorology and Climatology. A heat flux value of 87 mW/m<sup>2</sup> was also assigned at the bottom of the model for the calibration of the two-dimensional numerical model, and thus no field temperature was given to the geothermal discharge area. This heat flux value is concordant with data found in the literature. In the Alps area, values are usually lower than 90 mW/m<sup>2</sup>, and evaluated between 80 and 90 mW/m<sup>2</sup> around the Central Massifs (Medici and Rybach 1995). The rock thermal conductivity is also an important parameter to be selected for the simulation, because a variation of this parameter will notably modify simulated temperatures. Clark and Niblett (1956) studied the terrestrial heat flow in Swiss Alps and thermal conductivities of crystalline rocks. They showed that, among 23 gneiss samples, the thermal conductivity average value is 2.65 W/mK. For the model calibration, a thermal conductivity value for the Aiguilles



**Table 2** Comparison of observed/evaluated and imposed/simulated values for geological and geothermal boundary conditions for the two-dimensional model

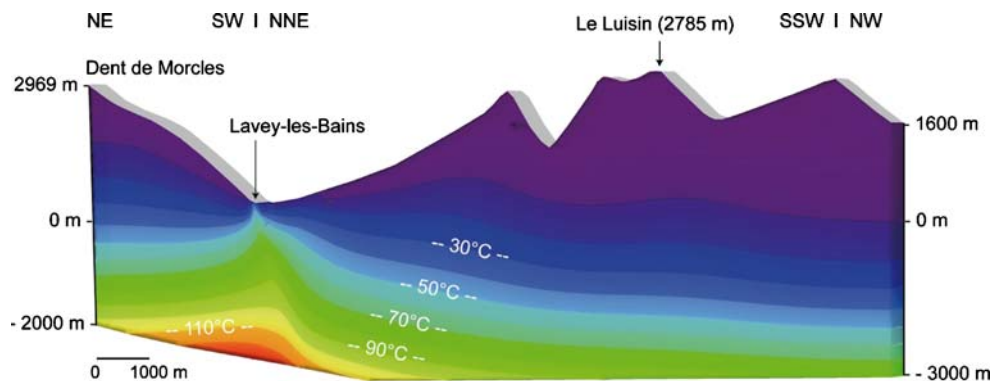
Boundary conditions	Observed-evaluated values	Imposed values
Water recharge (mountain condition)	1–20% of precipitation	10% of precipitation
Imposed head		Elevation of rivers
Hydraulic conductivity (m/s)		
Gneiss decompression zone	$>10^{-7}$	$2 \cdot 10^{-7}$
Deep gneiss	$10^{-6}$ – $10^{-12}$	$10^{-7}$ – $10^{-9}$
Fractured zone of gneiss	$10^{-1}$ – $10^{-4}$	$10^{-3}$
Glaciolacustrine deposits	$10^{-5}$ – $10^{-8}$	$10^{-6}$
Epinassey fan delta	$10^{-4}$ – $10^{-6}$	$10^{-5}$
Alluvial deposits	$10^{-2}$ – $10^{-4}$	$10^{-3}$
Conductivity anisotropy factor		
Deep gneiss	$K(x)/K(y) = 2$ and $75^\circ$	
Fractured zone of gneiss	$K(x)/K(y) = 10$ and $110^\circ$	
Glaciolacustrine deposits	$K(x)/K(y) = 10$ and $0^\circ$	
Porosity (%)		
Aiguilles Rouges gneiss	$<10$	$<10$
Quaternary deposits	1–20	5–15
Surface temperature ( $^\circ\text{C}$ )	0–9	0–9
Heat flux ( $\text{mW/m}^2$ )	80–90	87
Rock thermal conductivity [ $\text{K(W/m)}$ ]		
Aiguilles Rouges gneiss	2.65	2.5
Quaternary deposits	2	2
Pumping discharge (L/min)		
Annual average discharge		
P600	800	
P201	350	
AGEPP (awaited production rate)	1,500–4,500	1,500
Temperature in wells ( $^\circ\text{C}$ )		
P600 (before exploitation)	68	68.4
P201 (before P600 exploitation)	62	56.4
AP (before P201 exploitation)	44	40
Calculated temperature at depth ( $^\circ\text{C}$ )	100–110	110–130
Geothermal gradient ( $^\circ\text{C/km}$ )	15–20	17
Mean residence time of deep water (years)	$>8,000$ ( $^{14}\text{C}$ )	30,000

Rouges gneiss of 2.5 W/mK was imposed. For the Quaternary deposits, which mainly consist of clay and sandy clay, an average thermal conductivity of 2 W/mK was assigned (VDI-Richtlinien 2000).

#### Comparison with the natural state of the geothermal reservoir

The calibration of the model in steady state enables the heat anomaly at Lavey-les-Bains induced by the deep flow system to be reproduced (Fig. 7). Computed temperatures are close to the observed measurements in the P600 well

before its exploitation ( $68^\circ\text{C}$ ) and are similar to the current annual average temperature for the P201 well ( $57^\circ\text{C}$ ; Table 2). The difference in temperature is due to more cold-water inflow towards the P201 well from the decompressed zone of the Morcles area. In reality, this process is correct but less important than computed because the temperature of the P201 well before its exploitation probably was higher than  $62^\circ\text{C}$ . Moreover, computed temperatures at 10 m below the Quaternary deposits are close to  $40^\circ\text{C}$ . It agrees with measurements made in November 1970 in the old well AP ( $44^\circ\text{C}$  in Högl 1980) before the exploitation of the P201 well. The

**Fig. 7** Cross section of the Lavey-les-Bains geothermal system showing temperature distribution linked to the deep flow system

geothermal gradient varies along the cross section: the lowest value of gradient ( $16^{\circ}\text{C}/\text{km}$ ) is found below the recharge zone and the highest value corresponds to the Rhone Valley discharge zone due to the uprising of the deep fluid (Fig. 7). Computed temperatures of the inferred deep reservoir give  $110\text{--}130^{\circ}\text{C}$  and are close to the value calculated with chemical equilibrium of minerals and with geothermometers ( $100\text{--}110^{\circ}\text{C}$ ).

The two-dimensional steady-state model makes it possible to give a reasonable hydrodynamic picture of the thermal aquifer. The groundwater level has a rather low elevation below the Dent de Morcles because it was decided to limit flows inside the Morcles gneiss and, for this reason, the simulated geothermal gradient appears stronger. Subsurface circulations of the Petits Perrons and the Dent d'Emaney Massifs supply, on one hand, the groundwater of the highest valleys inside the decompressed zone and, on the other hand, the Lavey-les-Bains geothermal system from the deepest flows. Contrasts of permeability between the decompressed zone and the deep aquifer are responsible for high values of calculated exfiltration on the highest valleys (60% of the total infiltration). In this model, the Rhone Valley discharge is consequently equal to 40% of the total groundwater recharge ( $1.8\text{ m}^3/\text{day}/\text{m}$ ). This value appears to be low compared to the pumping rates in Lavey-les-Bains. But this result has to be multiplied by the width of the supposed watershed (approximately  $3,000\text{--}5,000\text{ m}$ ), meaning that a discharge of about  $5,400\text{--}9,000\text{ m}^3/\text{day}$  is obtained, 2–4 times higher than the maximum rate, which can be pumped ( $2,400\text{ m}^3/\text{day}$ ). However, it was possible to augment the Rhone Valley exfiltration by prolonging the cross section in the Aiguilles Rouges Massif and thus increasing the infiltration area. The water flux through the fractured zone below the Quaternary deposits has an important linear variation in function of depth. The flux at the bottom of the model is 50 times more important than at shallow depth.

Using the particle tracking option, the model gives an average residence time of the deepest fluid in the order of 30,000 years, higher than the carbon-14 evaluation ( $>8,000$  years). The carbon-14 evaluation is most probably influenced by a certain amount of mixing with recent and shallow groundwater. This computed value is dependant on the chosen low permeability value of the deep gneiss unit ( $10^{-8}\text{--}10^{-10}\text{ m/s}$ ).

#### Long-term effects of pumping rates on temperature

Additional pumping wells put into the two-dimensional model made it possible to forecast long-term effects of reservoir development on the temperature field. An unsteady state model was constructed from the annual average discharge of the two boreholes: 800 L/min for P600 and 350 L/min for P201. These pumping rates were corrected in the model from the evaluated width of the cone of influence of each well, because it is not appropriate to impose the real pumping rates of exploitation in a two-dimensional numerical model due to the

radial flow components out of the cross-section. The computed temperature decreases in the two boreholes due to additional contributions of cold waters from the Morcles gneiss (Fig. 8). The model shows a total loss of temperature of  $2^{\circ}\text{C}$  in P600 and of  $10^{\circ}\text{C}$  in P201, with stabilization after 100 years of exploitation. Nevertheless, observed values seem to indicate a stabilization of temperature after 2005, less than 10 years of production by the P600 well, and a final decrease of  $5^{\circ}\text{C}$  in the P201 well and  $3^{\circ}\text{C}$  for the P600 well. Consequently, the influence of cold-water inflows is more pronounced in the model than in reality. The local calibration of the unsteady state model is difficult because the two-dimensional model represent the regional flow system. Therefore, it is not appropriate to reproduce the local mixing process.

#### Outline of the two-dimensional model

The conception of a simplified two-dimensional numerical model from a regional NNE–SSW cross section through the Aiguilles Rouges crystalline Massif allowed for representation of the initial conditions of the Lavey-les-Bains deep flow system such as the temperature field below the Quaternary deposits and temperatures of the deep inferred reservoir. Nevertheless, the approximation of the uprising water flux is made difficult because the third dimension can not be taken into account due to the complexity of geological structures and the accentuated topography. The width of the watershed and its extension in the NNE–SSW direction, and the quantification of infiltration in the model, also are important parameters that are difficult to evaluate and have a significant influence on the estimation of the uprising water flux. Selected pumping rates gave computed temperatures, which overestimate additional contributions of cold waters from the Morcles gneiss.

Long-term temperature prediction for optimal management of the geothermal resource does not seem fully comparable to the reality. Even if the two-dimensional model correctly represents initial conditions, it is not

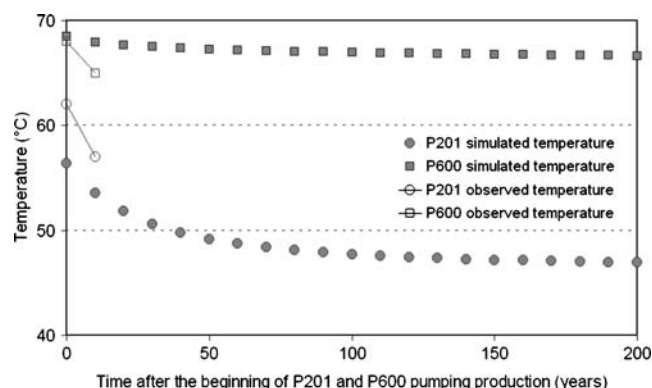


Fig. 8 Long-term simulated production temperature at the two wells compared with measured temperatures

suitable when new pumping rates are added. For this reason, a three-dimensional numerical model in the boreholes zone has to be considered.

### Three-dimensional local modelling of groundwater heat, flow and mass transport

Mixing conditions at shallow depth between cold water from the slope and deep thermal upflows are estimated from a three-dimensional local model of groundwater heat, flow and mass transport. Compared with the two-dimensional model, conservative chemical elements of various mixing end-members are used as natural tracers in addition to the temperature. It is important to specify that each used chemical parameter was directly calculated at the nodes where the flow rates are imposed. Water–rock interaction was not taken into account because the three-dimensional model is limited to a shallow depth zone with faster circulations. In this zone, variations of concentrations are mainly due to the mixing process between the two end-members.

Although the regional deep flow system is not illustrated on the three-dimensional model, it is possible to simulate the effects of pumping rates. Initial conditions of groundwater heat, flow and mass transport were calibrated by using temporal data from borehole measurements and results of the two-dimensional model. Desired aims are first to represent mixing conditions between different types of waters before and during the exploitation; second to simulate and to predict variations of physico–chemical parameters observed in the P201 well and third to imagine long-term effects of a new deep borehole (AGEPP project) on the geothermal resource.

#### Geological boundary conditions

The three-dimensional model structure is similar to a coarse rectangle of 100×600 m size with a 600 m depth, placed at 80 m below the bottom of well P600. It extends 200 m downstream from the P201 and 200 m upstream from the P600. The grid consists of 62,100 cells distributed uniformly on 54 layers (Fig. 9). The first three cell layers correspond to the Quaternary filling of the Rhone Valley including the recent Rhone alluvial deposits (coarse sandy gravels) and the glaciolacustrine sand and silt (Figs. 4 and 9). The other layers are assumed to be the fractured zone of gneiss and are considered equivalent to a porous medium. The interface between these two units was defined according to the data from boreholes and piezometers. This interface slopes towards the Rhone River and beneath the river, and an interface depth of 200 m is fixed, because in the middle of the valley the Quaternary filling reaches a thickness of about 500 m (Besson et al. 1993). Further from the river, at the hillside representing the edge of the model, the interface slope reaches an arbitrary depth of only 5 m (Fig. 9).

The six boundaries are represented by the top, the bottom and the four lateral sides of the model, assuming

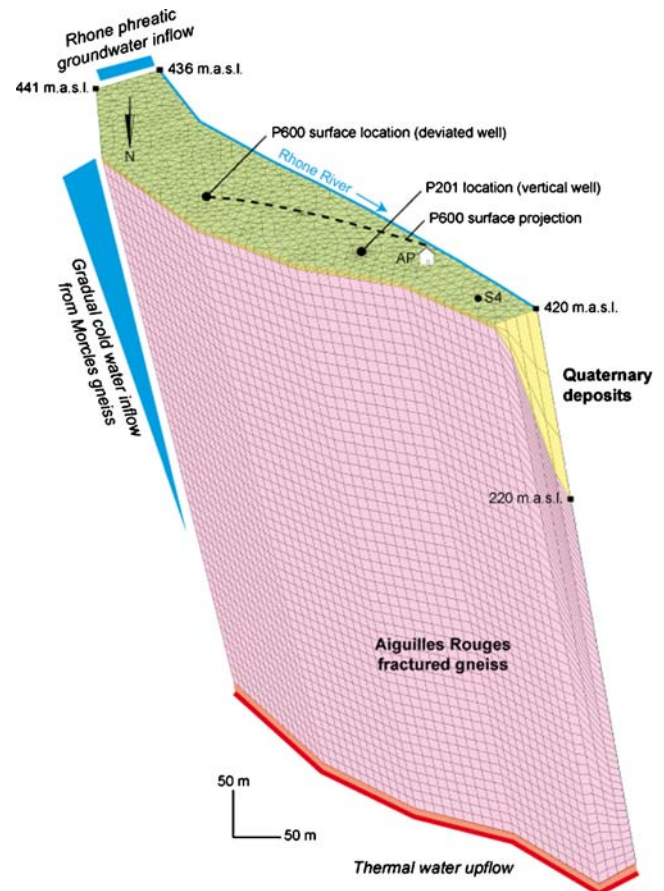
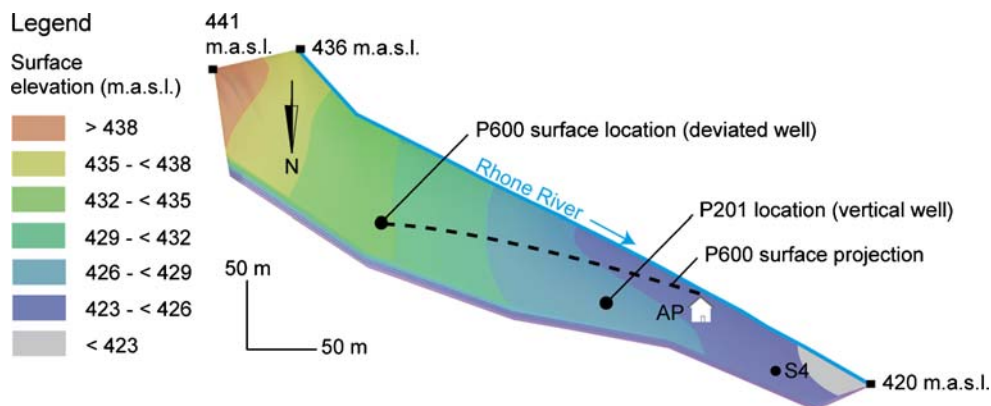


Fig. 9 Conceptual three-dimensional model of the Lavey-les-Bains geothermal system, showing the finite element mesh geometry used for the simulation and the initial boundary conditions (thermal inflow and cold water recharge)

that they are appropriate and justified. In detail, the description of each boundary is given below:

- The top of the domain represents the totality of the alluvial plain of the geothermal zone from the hillside to the Rhone River. The surface topography was constructed with the kriging option from data, and varies between 441 and 420 m.a.s.l. (Fig. 10).
- The bottom of the model is regarded as a plane surface with an elevation equal to 180 m below sea level, with an imposed thermal water flux. From the bottom, waters uprise towards the Rhone River.
- The northern and southern lateral sides are narrow (approximately 50 m) and support the Rhone phreatic groundwater inflow within the Quaternary filling from the south to the north.
- The eastern side corresponds to the vertical limit between the slope and the alluvial plain. It supports the gradual cold-water inflow from Morcles gneiss on all the high parts of its surface.
- The western side consists of the vertical prolongation of the Rhone River, which can be assumed as a hydrogeological barrier with no flow.





**Fig. 10** Constructed top surface topography for the three-dimensional model of the geothermal zone

Finally, the grid was refined in the vicinity of the two production wells to limit the potential numerical errors during the simulation. The size of the cells where flow rates are imposed is close to the diameter of the wells (approximately 30 cm).

#### Assigned parameters

For the calibration of the model, the necessary total flux of the uprising thermal water is  $5,454 \text{ m}^3/\text{day}$  and is homogeneously distributed on the totality of surface, that is to say 2.3 times more than the maximum production rate of the two wells ( $2,380 \text{ m}^3/\text{day}$ ). It also corresponds to 79% of total inflow in the model ( $6,860 \text{ m}^3/\text{day}$ ), knowing that the cold components coming from the slope and from the alluvial groundwater are approximately five times less important than the thermal component. The calculated water balance is slightly underestimated compared to the two-dimensional model simulation ( $5,400\text{--}9,000 \text{ m}^3/\text{day}$ ).

With regard to thermal inflow, a temperature of  $68^\circ\text{C}$  is imposed which corresponds to the pure thermal end-member, as measured in P600 well before production (G. Bianchetti, Alpgeo Ltd., unpublished data, 2002). A geochemical study undertaken within the framework of the AGEPP project showed that the pure thermal end-member at a depth of 600 m contains Cl,  $\text{SO}_4$  and Mg at respectively 265, 618 and  $0.3 \text{ mg/L}$  (unpublished data). In addition to the temperature, these three ions, which have certainly limited precipitation/dissolution reactions in the mixing zone due to fast circulation, are used as natural tracers to represent these mixing conditions. For cold inflow, a temperature of  $9^\circ\text{C}$  was imposed for the alluvial aquifer and a range of  $9\text{--}20^\circ\text{C}$  for the slope groundwater. Chloride, sulphate and magnesium imposed concentrations are respectively 3, 67 and  $12 \text{ mg/L}$  according to extrapolation from chemical analyses of all sampling points (unpublished data).

Finally, imposed conditions for rock permeability, anisotropy factors and thermal conductivities remained similar to the conditions of the two-dimensional model. Concerning the fault zone, which was considered equiv-

alent to a porous environment, high hydraulic conductivities in particular on the vertical axis Z are assigned (use of hydraulic conductivity anisotropy factor option in the FEFLOW code). Values of hydraulic conductivities on horizontal directions X and Y are equivalent ( $1.10^{-4} \text{ m/s}$ ) and 100 times higher on Z ( $1.10^{-2} \text{ m/s}$ ) due to the presence of opened vertical fractures. For the Rhone alluvial deposits imposed conductivities are  $1.10^{-3} \text{ m/s}$  on X and Y, and  $1.10^{-4} \text{ m/s}$  on Z according to interpretation of pumping tests (D. Blant, CHYN, unpublished data, 1992).

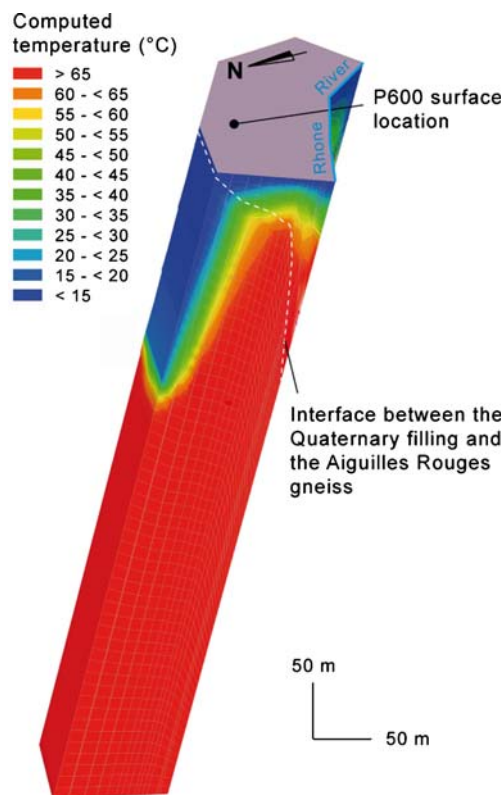


**Fig. 11** Three-dimensional simulation of the initial background temperature field before production

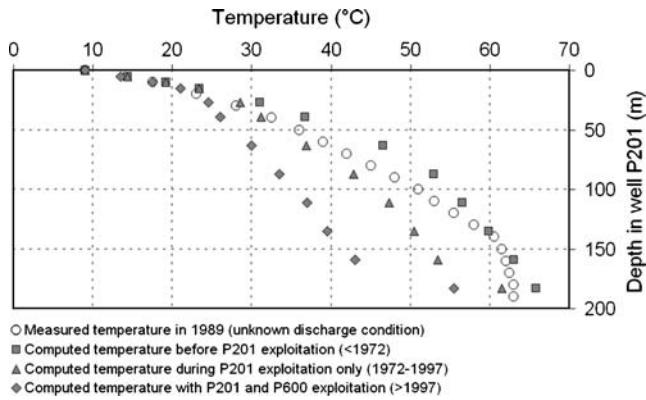


**Fig. 12** Comparison of computed and measured temperature profiles in the P201 well

#### Discussion of four simulation scenarios

Four scenarios are investigated with steady state and transient models. They present the exploitation history since the installation of the first deep P201 well in 1972. First, the background temperature field and initial mixing conditions are established in the absence of pumping rates (before P201). In a second scenario, the temperature distribution and the chemical contents are computed with the exploitation of the P201 well (before P600). Then, long-term effects of the P600 well on the P201 production are predicted (before AGEPP project). Finally, the future deep AGEPP borehole is added into the three-dimensional model to show its possible impact on production of the P201 and P600 wells.

- *First scenario: During production of the deep AGEPP borehole (probably after 2010).* The steady-state three-dimensional model without pumping wells made it possible to approximate the initial background temperature field via a cross section between P201 and P600 (Fig. 11), and represents the initial aquifer concentrations for the simulations with pumping wells. At a given depth (for example 50 m), the temperature below the Quaternary filling increases from the hillside to the river and then slightly decreases with the sediments due to a permeability contrast. Computed temperatures are acceptable compared to the measurements made before 1972 in AP and during the drilling of the P201 before its exploitation (Fig. 12 and Table 3).

- *Second scenario: During P201 exploitation only (1972–1997).*

The second scenario highlights the effects on the geothermal field due to the pumping rate of P201 only, with an annual average discharge at 300 L/min. During this time interval, P600 is not yet present and the exploitation of the thermal aquifer is supplied by P201 only, and beyond 1997, P201 exploitation continues with P600. The decrease of simulated temperatures from 65.8 to 61.5°C is satisfactory compared to the recorded data (Fig. 13 and Table 3). This decline is associated with an increase of the mixing ratio as shown by computed concentrations of chemical tracers: Cl=238 mg/L, SO<sub>4</sub>=564 mg/L and Mg=1.5 mg/L. These values represent, at the P201 well, the initial aquifer concentrations before the simulation with the P600 production rate (first concentration points on the Fig. 13). Using imposed concentrations, the mixing ratio during the P201 exploitation is estimated at 10% for cold waters and 90% for the thermal component. Finally, simulated temperatures in the old well do not correspond to observed data (42°C simulated instead of 22–36°C measured). In the three-dimensional model, the Rhone alluvial groundwater circulates mainly in Quaternary deposits, whereas characteristics of this shallow well (28 m including 18 m inside sediments) support alluvial groundwater inflows inside the well due to a drawdown of the thermal water hydraulic head.

- *Third scenario: Effects of P600 exploitation on P201 (after 1997).*

In a third scenario, the P600 deeper well is added to the system with an annual average pumping rate of 800 L/min. Its position close to the bottom section of P201 causes a decrease of the hydraulic head of the uprising thermal water and favours additional cold-water inflows (Fig. 13). Electrical conductivity and temperature measurements taken in P201 since the exploitation of P600 clearly showed a dilution of P201 thermal water and modelled results reproduce these observations. The calibration of the model made it possible to validate the first estimation of the long-term temperature behaviour: time necessary to stabilize the temperature in P201 from 61.5°C in 1997 to 56°C takes 10 to 15 years.

With regard to the variation of the chemical tracers computed by the model (Fig. 13), the pumping rate in P600 induces a reduction in chloride and sulphate concentrations (respectively 204 and 494 mg/L) and an increase of magnesium concentration (3 mg/L). Consequently, the mixing ratio between cold and thermal waters

**Table 3** Comparison of computed and measured temperatures in three Lavey-les-Bains wells according to four simulation scenarios

	Background field temperature (<1972)		P201 exploitation (1972–1997)		P600 exploitation added (>1997)		AGEPP production added (probably >2010)	
	MT	CT	MT	CT	MT	CT	MT	CT
Well								
P600	–	68	–	68	65	67.5	–	66–67
P201	63–65	65.8	62	61.5	57	55.7	–	39–41
AP	44	43	22–36	42	18–22	39	–	–

MT measured temperature (°C); CT computed temperature (°C)

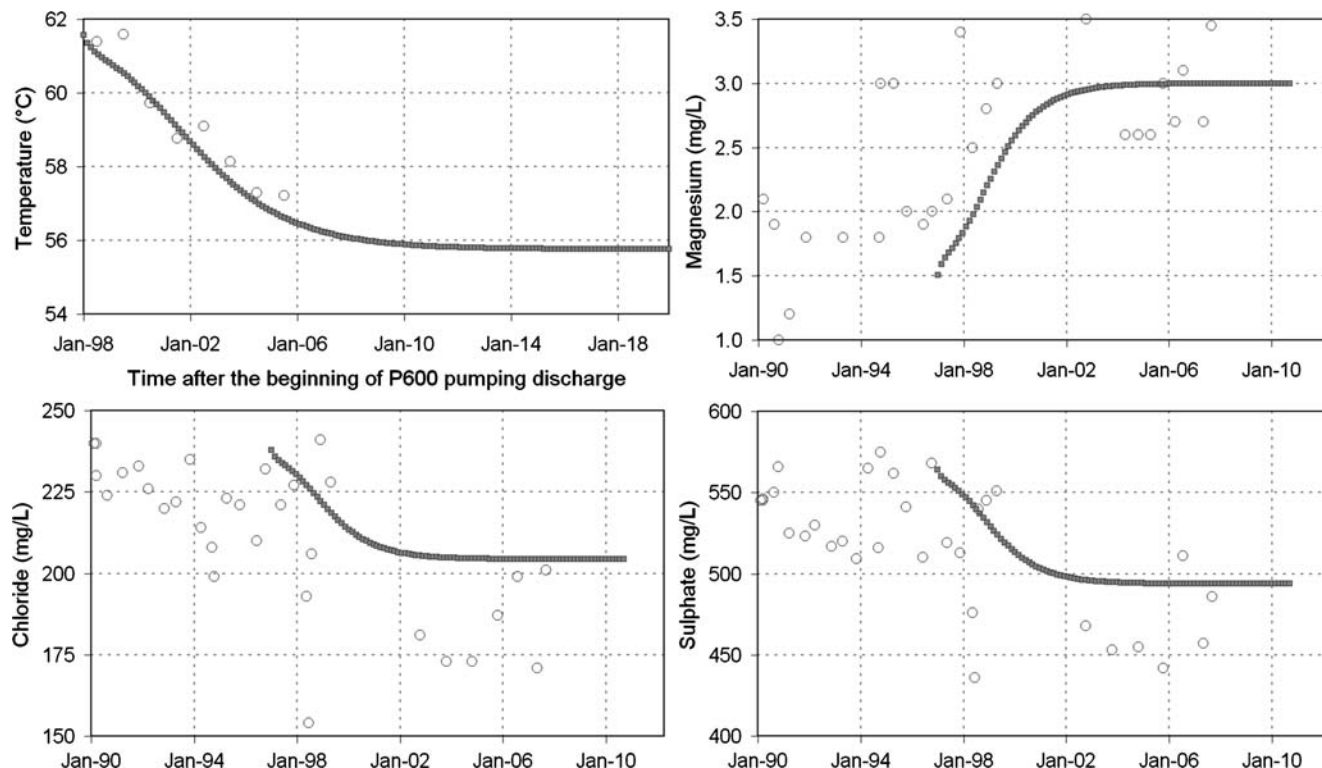


**Fig. 13** Comparison of computed (squares) and measured (circles) physico-chemical parameters in P201 well after production in P600 well started in 1997

evolves from 10/90 to 23/77%. Finally, due to the structure of the three-dimensional model and to the position of the deep P600 well close to the thermal inflow, it was not possible to reproduce the temperature decrease in P600 (67.5°C computed instead of 65°C observed in 2007).

- *Fourth scenario: Effects of P600 exploitation on P201 (after 1997).*

In a last scenario, it was decided to simulate the possible impact of the future deep AGEPP borehole on the existing production wells. Inferring that the AGEPP borehole will reach at least 2,000 m below the three-dimensional model, the employed method decreases fluxes uprising at the bottom of the model. Initially, the total imposed value of fluxes at the bottom of the model was 5,454 m<sup>3</sup>/day or 63 L/s. It appears insufficient for the objectives of the AGEPP project (50–75 L/s). It is impossible to simulate an exploitation rate higher than 63 L/s because thermal upflows will be absent in the model. For this reason, a flow rate of 25 L/s was selected for the simulation and is more appropriate for this model than a flow rate of 50 L/s which would generate stronger cold-water inflows in wells. It is difficult to appreciate if the AGEPP project overestimates the geothermal potential, or if the calculated total flow at the bottom of the model is underestimated.

The temperature variation shows a major reduction in P201 (more than 15°C), with a stabilization at 40°C after 20–25 years of exploitation (Fig. 14). Concerning P600, a decrease of the production yield may be possible but

probably less important than for P201, because of a lower variability of the physico-chemical parameters in P600, being less subject to the mixing process by cold-water inflow. In the case of a significant decrease of the production rates in the P600 and P201 wells, it could be envisaged that water pumped by the AGEPP borehole could be used after extraction of the energy.

## Conclusions

The exploitation of the P600 well causes dilution of the thermal water in the P201 well by shallow cold ground-water from the gneissic Morcles Massif. It was thus

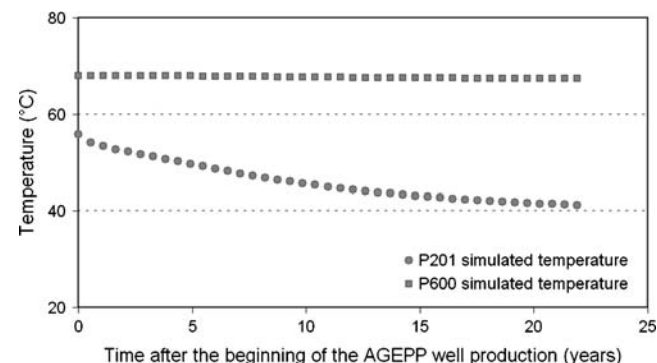


**Fig. 14** Temperature simulation of the two existing production wells during the exploitation of the future deep well AGEPP at a rate of 25 L/s



important to decipher these mixing processes with chemical investigations and models, and to estimate the long-term behaviour of physico-chemical parameters for optimal management of the geothermal resource.

Continuous measurements of physico-chemical parameters in P201 and P600 waters and discrete measurements on several sampling points made it possible to highlight mixing processes. Initially, a two-dimensional model of groundwater flow and heat transport within a regional cross section of the Aiguilles Rouges Massif partly reconstituted the observed geothermal anomaly below the Rhone Valley (computed temperatures of 68, 56 and 40°C respectively in the P600, P201 and AP wells), and gave a temperature of the deep inferred reservoir of 100–130°C. The simulated thermal water flux (5,400–9,000 m<sup>3</sup>/day) corresponds to 2–4 times the maximum production rate (2380 m<sup>3</sup>/day) and seems to be underestimated. The watershed probably extends towards the south-western part of the Aiguilles Rouges Massif.

Then, a three-dimensional local model on a perimeter including all the Lavey-les-Bains sampling points was realized, considering the same assigned parameters as in the two-dimensional model. The thermal water flux used is comparable to the one obtained with the two-dimensional model (5,454 m<sup>3</sup>/day). Different simulation scenarios using the average annual discharges of P600 and P201 wells and some natural chemical tracers, made it possible to calculate the mixing ratios comparable with those estimated in the P201 well (10/90% before the P600 well and 23/77% with the P600 exploitation). Moreover, long-term effects on P201 could be defined with the three-dimensional model. Computed and measured temperatures are concordant and illustrate a stabilization of the temperature at 56°C after 10 to 15 years of production at the P600 well. According to the model, a future exploitation of the deep inferred reservoir with pumping rates of 25–75 L/s may induce a significant decline of thermal output in the two existing wells in Lavey-les-Bains.

**Acknowledgements** Special thanks are given to G. Bianchetti (Alpgeo Ltd.) for providing data for the studied site and for his agreement to quote the AGEPP project in this report. We also address our sincere gratitude to Prof. Pierre Perrochet, from the Swiss Center for Hydrogeology (CHYN University of Neuchâtel, Switzerland), who validated the concepts and results of the numerical modelling.

## References

- André L, Rabemanana V, Vuataz FD (2006) Influence of water–rock interactions on fracture permeability of the deep reservoir at Soultz-sous-Forêts, France. *Geothermics* 35(5):507–531
- Besson O, Marchant R, Pugin A, Rouiller JD (1993) Campagne de sismique-réflexion dans la vallée du Rhône entre Sion et Saint-Maurice: perspectives d'exploitation géothermique des dépôts torrentiels sous-glaciaires [Seismic-reflection investigation in the Rhone Valley between Sion and Saint-Maurice: prospects for geothermal exploitation of the subglacial torrential deposits]. *Bull CHYN* 12:39–58
- Bianchetti G (1994) Hydrogéologie et géothermie de la région de Lavey-les-Bains (Vallée du Rhône, Suisse) [Hydrogeological and geothermal characteristics of the Lavey-les-Bains area (Rhône Valley, Switzerland)]. *Bull Hydrogéol* 13:3–32
- Clark SP, Niblett ER (1956) Terrestrial heat flow in the Alps. *Mon Not R Astro Soc* 7:176–195
- Cruchet M (1985) Influence de la décompression sur le comportement hydrogéologique des massifs cristallins en Basse Maurienne (Savoie, France) [Influence of the decompression on the hydrogeological behaviour in the Basse Maurienne crystalline Massifs (Savoy, France)]. *Géol Alp* 61:65–73
- Dobson PF, Salah S, Spycher N, Sonnenthal EL (2004) Simulation of water–rock interaction in the Yellowstone geothermal system using TOUGHREACT. *Geothermics* 33(4):493–502
- Flores-Márquez EL, Jiménez-Suárez G, Martínez-Serrano RG, Chávez RE, Silva Pérez D (2006) Study of geothermal water intrusion due to groundwater exploitation in the Puebla Valley aquifer system, Mexico. *Hydrogeol J* 14(7):1216–1230
- Gevrek AI (2000) Water/rock interaction in the Kizilcahamam Geothermal Field, Galatian Volcanic Province (Turkey): a modelling study of a geothermal system for reinjection well locations. *J Volcanol Geotherm Res* 96(3–4):207–213
- Högl O (1980) Die Mineral- und Heilquellen der Schweiz [Mineral and thermal resources in Switzerland]. Haupt, Bern, Switzerland, 302 pp
- Kohl T, Evans KF, Hopkirk RJ, Rybach L (1995) Coupled hydraulic, thermal and mechanical considerations for the simulation of hot dry rock reservoirs. *Geothermics* 24(3):345–359
- Kolditz O, Clauser C (1998) Numerical simulation of flow and heat transfer in fractured crystalline rocks: application to the Hot Dry Rock site in Rosemanowes (U.K.). *Geothermics* 27(1):1–23
- Kühn M, Stöfen H (2004) A reactive flow model of the geothermal reservoir Waiwera: New Zealand. *Hydrogeol J* 13(4):606–626
- Leaver JD, Unsworth CP (2007) System dynamics modelling of spring behaviour in the Orakeikorako geothermal field, New Zealand. *Geothermics* 36(2):101–114
- Lhomme D, Dzikowski M, Nicoud G, Payraud B, Fudral S, Guillot PL (1996) Les circulations actives des eaux souterraines des massifs cristallins alpins: exemple des Aiguilles Rouges (Haute-Savoie, France) [Groundwater circulation systems of Alpine crystalline massifs: the Aiguilles Rouges case]. *CR Acad Sci Paris* 323(2):681–688
- Maréchal JC (1998) Les circulations d'eau dans les massifs cristallins alpins et leur relations avec les ouvrages souterrains [Water circulations in the Alpine crystalline massifs and their relations with tunnels]. Paper no. 1769, EPFL, Lausanne, Switzerland, 296 pp
- Maréchal JC (1999) Observation des massifs cristallins alpins au travers des ouvrages souterrains. Définition du rôle hydrogéologique de la zone décompressée [Observation of Alpine crystalline massifs through tunnels: definition of the hydrogeological role of the decompressed zone]. *Hydrogéologie* 1:33–42
- McDermott CI, Randriamanjatoa ARL, Tenzer H, Kolditz O (2006) Simulation of heat extraction from crystalline rocks: the influence of coupled processes on differential reservoir cooling. *Geothermics* 35(3):321–344
- Medici F, Rybach L (1995) Geothermal map of Switzerland 1995 (Heat flow density), Matér géol Suisse, Géophys 30:1–36
- Nicholson K (1993) Geothermal fluids: chemistry and exploration techniques. Springer, Berlin, 263 pp
- Parriaux A, Nicoud G (1993) Les formations glaciaires et l'eau souterraine [Glacial formations and groundwater]. *Quaternaire* 4(2–3):61–67
- Pfiffner OA, Lehner P, Heitzmann P, Mueller S, Steck A (1997) Deep structure of the Swiss Alps. Results of NRP 20. Birkenhäuser, Basel, Switzerland, 380 pp
- Porrás EA, Tanaka T, Fujii H, Itoi R (2007) Numerical modeling of the Momotombo geothermal system, Nicaragua. *Geothermics* 36(4):304–329

- Pruess K (2006) Enhanced geothermal systems (EGS) using CO<sub>2</sub> as working fluid: a novel approach for generating renewable energy with simultaneous sequestration of carbon. *Geothermics* 35(4):351–367
- Sonney R, Vuataz FD (2008) Properties of geothermal fluids in Switzerland: a new interactive database. *Geothermics* 37(5):496–509
- Teng Y, Koike K (2007) Three-dimensional imaging of a geothermal system using temperature and geological models derived from a well-log dataset. *Geothermics* 36(6):518–538
- VDI-Richtlinien (2000) Thermal use of the underground: fundamentals, approvals and environmental aspects, part 1. VDI4640, Beuth, Berlin, 32 pp
- Von Raumer JF, Bussy F (2004) Mont Blanc and Aiguilles Rouges geology of their polymetamorphic basement: external massifs, Western Alps, France-Switzerland. *Mém Géol (Lausanne)* 42, 203 pp
- Vuataz FD (1982) Hydrogéologie, géochimie et géothermie des eaux thermales de Suisse et des régions alpines limitrophes [Hydrogeological, geochemical and geothermal characteristics of thermal waters in Switzerland and the bordering Alpine areas]. *Matér Géol Suisse, Sér Hydrol* 29:174
- Zahner P, Mautner J, Badoux H (1974) Etude hydrogéologique des sources thermominérales de Lavey, d'Yverdon et de Saxon [Hydrogeological study of mineral and thermal springs of Lavey, Yverdon and Saxon]. *Mém Soc Vaud Sci Nat* 95(15):209–234